Original Article
http://dx.doi.org/10.5115/acb.2016.49.1.21
pISSN 2093-3665 eISSN 2093-3673
Anatomy & Cell Biology acb

Modulation of axonal sprouting along rostro-caudal axis of dorsal hippocampus and no neuronal survival in parahippocampal cortices by long-term post-lesion melatonin administration in lithium-pilocarpine model of temporal lobe epilepsy

Mahsa Kazemi[1], Saeed Shokri[2], Mahin Ganjkhani[1], Rostami Ali[1], Jafari Anarkooli Iraj[2]
Departments of [1]Physiology and [2]Anatomical Sciences, Faculty of Medicine, Zanjan University of Medical Sciences, Zanjan, Iran

Abstract: Feature outcome of hippocampus and extra-hippocampal cortices was evaluated in melatonin treated lithium-pilocarpine epileptic rats during early and chronic phases of temporal lobe epilepsy (TLE). After status epilepticus (SE) induction, 5 and 20 mg/kg melatonin were administered for 14 days or 60 days. All animals were killed 60 days post SE induction and the histological features of the rosrto-caudal axis of the dorsal hippocampus, piriform and entorhinal cortices were evaluated utilizing Nissl, Timm, and synapsin I immunoflorescent staining. Melatonin (20 mg/kg) effect on CA1 and CA3 neurons showed a region-specific pattern along the rostro-caudal axis of the dorsal hippocampus. The number of counted granular cells by melatonin (20 mg/kg) treatment increased along the rostro-caudal axis of the dorsal hippocampus in comparison to the untreated epileptic group. The density of Timm granules in the inner molecular layer of the dentate gyrus decreased significantly in all melatonin treated groups in comparison to the untreated epileptic animals. The increased density of synapsin I immunoreactivity in the outer molecular layer of the dentate gyrus of untreated epileptic rats showed a profound decrease following melatonin treatment. There was no neuronal protection in the piriform and entorhinal cortices whatever the melatonin treatment. Long-term melatonin administration as a co-adjuvant probably could reduce the post-lesion histological consequences of TLE in a region-specific pattern along the rostro-caudal axis of the dorsal hippocampus.

Key words: Status epilepticus, Melatonin, Temporal lobe epilepsy, Hippocampus

Received September 3, 2015; Revised December 16, 2015; Accepted December 24, 2015

Corresponding authors:
Mahin Ganjkhani
Department of Physiology, Faculty of Medicine, Zanjan University of Medical Sciences (ZUMS), Zanjan, P.O. Box 45139-56184, Iran
Tel: +98-24-33440301, Fax: +98-24-33449553, E-mail: ghanjkhani@zums.ac.ir
Saeed Shokri
Department of Anatomical Sciences, Faculty of Medicine, Zanjan University of Medical Sciences (ZUMS), Zanjan, P.O. Box 45139-56184, Iran
Tel: +98-24-33440301, Fax: +98-24-33449553, E-mail: saeedshus@zums.ac.ir

Introduction

Temporal lobe epilepsy (TLE), as the most common type of epilepsy in adults, arises from abnormalities in the temporal lobe (the amygdala, the hippocampus and the temporal cortex) [1]. Following an initial precipitating injury, various cellular and molecular changes occur in the temporal lobe. The hippocampus and the parahippocampal areas undergo

both neuronal and interneuronal loss in addition to reactive gliosis. Other features remodeling such as axonal or dendritic reorganization, granule cell layer (GCL) dispersion and the appearance of ectopic granule cells are common in epileptic hippocampus [1]. These kind of abnormalities cause neurobiological, cognitive, psychological, and social consequences in epileptic patients [2]. The majority of patients with hippocampal sclerosis have intractable seizures that cannot be well controlled with classical anticonvulsant drugs [3, 4]. Hence, there is a compelling need to find a new drug or co-adjuvant for reducing the pathological and social consequences of TLE.

Melatonin, as a major secretory product of the pineal gland, can affect the central nervous system through different pathways. It is a modulator of the neuroimmunoendocrine system [5]. As a putative free radical scavenger and antioxidant [6], it is also able to alter the activities of antioxidant enzymes [7]. Melatonin enhances either the content or expression of neurothrophic factors [8]. This neurohormone plays a critical role in neurogenesis [9, 10]. Evidence indicates that melatonin has an important action as a cytoskeletal modulator and a neurite outgrowth stimulator in neuronal cells as well [11, 12].

During the last two decades, many studies have been conducted to find out the different effects of melatonin on TLE. Melatonin showed anticonvulsant properties in animal models of TLE [13, 14]. Acute administration of this neurohormone before and 2 hours continuously after status epilepticus (SE) induction showed the antioxidant and anti-inflammatory properties of melatonin against kainic acid (KA)–induced hippocampal neurodegeneration [15]. De Lima et al. [16] have shown the neuroprotective effect of melatonin in pinealectomized epileptic rats which received melatonin before and over 2 hours after SE induction in the pilocarpine model. Lee et al. [17] focused on the underlying protective mechanism of melatonin against neuronal death in the hippocampus by administrating it 1 hour prior to KA-induced SE. Since, the potential protective effect of melatonin after the onset of SE was not clear, Lima et al. [14] showed the neuroprotective effect of melatonin by attenuating SE-induced post-lesion and promoting a decrease in the number of seizures in epileptic rats that were treated for 30 minutes over 48 hours after pilocarpine-induced SE. On the other hand, TLE is a chronic inflammatory process in the central nervous system [12, 18]. Although most neuropathological changes that trigger epileptogenesis occur at the early period after the precipitating injury [15], the greater part of pathohistological remodeling in the SE induced injured hippocampal and parahipocampal areas, especially mossy fiber sprouting and neuronal network remodeling that trigger epileptogenesis, occur during a long time lapse post SE [13, 19]. On the other hand, it was shown that even 1- and 10-hour topiramate injection post SE as an approved anti-convulsant drug could not stop mossy fiber sprouting as a marker of the epileptogenesis process [20-22]. Based on recent video-electroencephalogram seizure monitoring and histological studies, 14 days were assumed as an appropriate time frame for the occurrence of the most part of pathohistological remodeling, specifically aberrant axonal sprouting and neurogenesis, in the SE induced injured hippocampal and parahipocampal areas [23, 24]. As the consequences of long-term morphological outcomes (specifically axonal sprouting) of melatonin administration remains ambiguous, we designed a histomorphometrical time window and dose dependent study to evaluate long outcome of melatonin treatment on the rostro-caudal axis of the dorsal hippocampus and the parahippocampal areas as the most vulnerable areas post SE [25-27].

Materials and Methods

Experimental procedures

All animal experiments were conducted in accordance with the national guidelines and protocols approved by the Institutional Animal Ethic Committee (IAEC No. 03/028/07). All experimental protocols were approved by the Zanjan University of Medical Sciences (ZUMS) ethics committee. Healthy adult male albino rats of the Wistar strain weighing 250 g were housed under environmentally controlled conditions in a 12/12-hour light/dark cycle. Standard laboratory diet (Pars Dam Co., Tehran, Iran), and clean drinking water was made available *ad libitum*.

Animal model of TLE

Briefly, methylscopolamine-bromide (1 mg/kg, subcutaneously; Sigma, St. Louis, MO, USA) was injected 30 minutes prior to pilocarpine administration. Following pilocarpine injection, seizure activity was monitored behaviorally and graded according to Racine's criterion [28]. A seizure severity grade was assigned according to a modified Racine scale previously reported [29]. The animals' maximal behavioral response was graded as follows: grade 0, no response; grade 1, wet dog shake (WDS) and/or behavioral

arrest; grade 2, WDS, staring, pawing, and chronic jerks; grade 3, WDS, staring, pawing, chronic jerks, rearing and falling; grade 4, continuous grade 3 seizures for more than 30 minutes (SE). Only rats that displayed continuous and convulsive seizure activities of stage 4 and 5 of Racine's criterion after pilocarpine injection were used in the experiments. SE onset was defined as the occurrence of continuous motor-limbic seizures accompanied by intermittent rearing and falling (grade 4 or 5 on the Racine scale) without returning to the normal behavior between seizures. For animals that developed SE, we controlled SE duration as 120 minutes by injecting diazepam (4 mg/kg, intramuscularly). In order to prolong animal survival period, they were kept at 4°C environmental temperature throughout the second hour of SE induction. The animals received the first melatonin injection exactly 2 hours after SE onset. The time of melatonin injection was chosen to be at the end of daylight time (18:00 hour).

Treatment

The test subjects were divided into seven groups: group A (control, n=6), untreated animals; group B (epilepsy, n=7), animals that exhibited 2 hours SE; group C (vehicle, n=7), SE induced animals that received the solvent of melatonin; group D (5 mg/60 days, n=7), SE induced animals that received melatonin (intraperitoneal, 5 mg/kg) for 60 days; group E (5 mg/14 days, n=6), SE induced animals that received melatonin (intraperitoneal, 5 mg/kg) for 14 days; group F (20 mg/60 days, n=7), SE induced animals that received melatonin (intraperitoneal, 20 mg/kg) for 60 days; group G (20 mg/14 days, n=7), SE induced animals that received melatonin (intraperitoneal, 20 mg/kg) for 14 days. Since the cell death and inflammation parallel spatial specificity of plastic changes throughout the epileptic brain after seizure [1, 6], we chose 14 and 60 days as the appropriate time courses of hippocampal remodeling after SE induction. On the other hand, as the cell proliferation in the pilocarpine-induced SE model increases within 3 days after SE and persists for at least 2 weeks [30], we limited the melatonin treatment either at 14 or 60 days after SE induction.

Morphological analysis

After deep anesthesia with ketamine (45 mg/kg) and xylasine (35 mg/kg), each rat was perfused transcardially with 200 ml of sodium sulfide perfusion medium (2.925 g Na_2S, 3 g NaH_2PO_4; H_2O in 500 ml distilled H_2O) and 200 ml of 4% paraformaldehyde that contained 0.1% glutaraldehyde consecutively. The brains were paraffin embedded following processing. Coronal sections through the entire extent of the hippocampus were cut at 5 μm on a microtome [31]. Every fourth section was chosen for mossy fiber staining based on the Timm method. Alternate sections were stained with cresyl violet for neuronal cell body quantification. In addition, another series of sections were stained with synapsin I marker.

Quantitative and descriptive analysis of neuronal damage

Nissl staining was performed on 5-μm-thick coronal sections which had been taken through the hippocampus and the parahippocampal cortices using the rat atlas [31]. In the stained sections, hippocampal and parahippocampal neurons were counted. Cells count involved only somas larger than 10 μm. for the rostral part of the dorsal hippocampus, coronal sections were collected from –3.3 from bregma extended rostrally to the anterior end of the dentate gyrus. For the rostral part of the dorsal hippocampus and piriform cortex, serial sections were collected –4.1 from bregma to –4.5. About –6.3 from bregma were chosen as ventral hippocampus and entorhinal cortex. Each location was identical in each processed brain block. For each animal, the average number of neuronal profiles in a given region was assessed in 3 separate sections by an observer not aware of the animal's treatment. The value per each section was the average of at least three values from two to three adjacent sections.

Quantification of cell density was performed with Image J software by placing a grid on a well defined area of the cerebral structure. Microscopic enlargement for each single cerebral structure and cell counts were performed based on Rigoulot et al. [21]. Values were expressed as mean±SEM.

According to a previous study [25], there is a striking heterogeneity in the extent of principal cell loss among animals studied 1 month after SE. For finding a probable similar trend between the aberrant axonal sprouting and the extent of cell death, we tried to score the cumulative damage scores of hippocampus according to Danzer et al. [25]. Cell loss was scored under 10× magnifications in four regions [25]: the hilus, dentate GCL, CA3 pyramidale cell layer, and CA1 pyramidale cell layer. The semiquantitative scored system was as follows: 0, no obvious cell loss; 1, less than 25% cell loss; 2, 50% cell loss; and 3, greater than 90% cell loss. Three adjacent hippocampal sections per animal were scored. The scores for each region were averaged and a cumulative cell loss score was given to the animal (cumulative cell loss= hilus+dentate+CA3+CA1; minimum possible score=0,

http://dx.doi.org/10.5115/acb.2016.49.1.21

maximum=12).

Timm histochemistry

Briefly, the sections were developed in the dark for 40–45 minutes in a Timm staining solution. The soulution consists of 50% (w/v) arabic gum (160 ml), 2 M sodium citrate buffer (30 ml), 5.7% (w/v) hydroquinone (80 ml), and 10% (w/v) silver nitrate (2.5 ml). The sections were rinsed with tap water at 40°C, then rinsed rapidly with distilled water and allowed to dry. They were then dehydrated in ethanol and cover slipped [21].

Quantification of distribution of Timm granules

The distribution of Timm granules in the supragranular layer (SGL) of the dentate gyrus and CA3 were evaluated by both computer assisted density measurements and scoring system that have been used previously in assessing sprouting [32]. The scoring system in the dentate gyrus: score of 0, absence of Timm granules in the SGL; 1, occasional granules or sparse distribution in the SGL; 2, several granules not continuously distributed in the SGL; 3, Timm granules almost continuously distributed in the SGL; 4, dense laminar band of granules almost continuous in the SGL; and 5, a dense band continuously distributed in the SGL of the dentate gyrus. Semiquantitative scaling system in the CA3 subfield: 0, no granules in the stratum pyramidale (SP) or stratum oriens (SO) along any portion of the CA3 subregion: 1, occasional granules in the SO or SP occurring in discrete bundles; 2, occasional to moderate granules in the SO or SP; 3, prominent granules in the SO or SP; 4, prominent granules in the SO or SP occurring in near-continuous distribution along the entire CA3 region; and 5, continuous or near-continuous dense laminar band of granules in the SO or SP along the entire CA3 region. Computer assisted density measurements of Timm staining in the dentate gyrus and CA3 subfields was performed according to previous studies [32, 33]. On average, 6 sections of the hippocampus per rat were examined. The density measurements were performed by Image J software (Fig. 1). A modified method used by Van der Zee et al. [33] was used [32]. In brief, images were captured digitally to a monitor. Light intensity and filter settings were maintained at a constant level for all specimens. Captured images were converted to gray scale. We placed circles sequentially in the SP at the junction between the SP and SO. Sequential circles were placed over the dentate GCL in both the inferior and superior blades and the three bands of the molecular layer. Once all circles were in place, a mean optical density was obtained. The maximum density value range in this system was 256.

Immunofluorescent labeling for synapsin I

The sections were incubated for 2 hours with blocking buffer (2% horse serum, 1% bovine serum albumin, 0.1% Triton X-100 in phosphate buffered saline, pH 7.5), overnight at 4°C with antisynapsin I antibody (1:1000, ab59268, Abcam, Cambridge, MA, USA). Then they were incubated for 1 hour at room temperature with fluorescein isothiocyanate–conjugated goat polyclonal secondary antibody to rabbit IgG-Fc (1:300, ab97199, Abcam). Finally, slides were coverslipped with Vectasheild hardest mounting medium

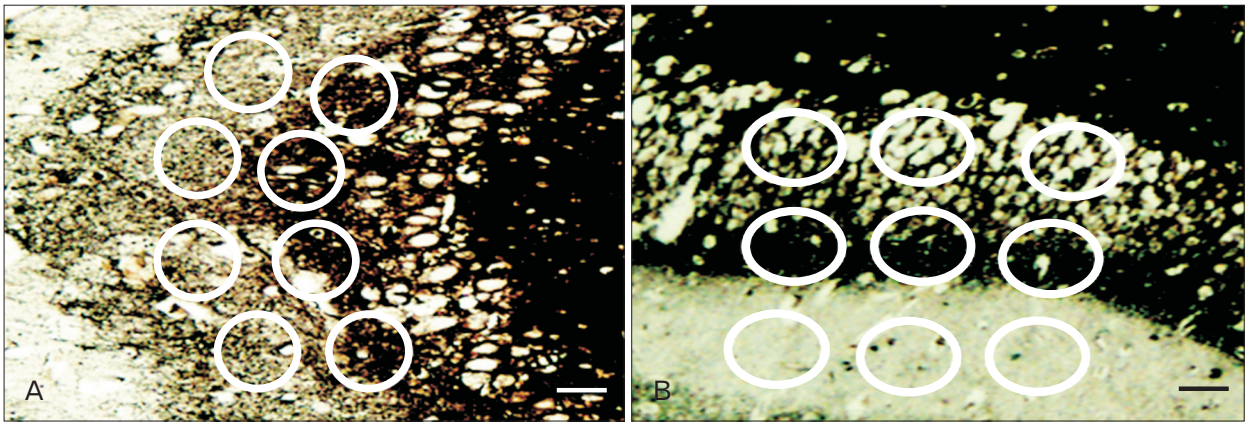

Fig. 1. (A) Location of circles placed sequentially along the junction between the stratum pyramidale and stratum oriens. If artifact or disrupted tissue was noted, the circles were placed on immediately adjacent tissue. (B) Location of circles placed over the dentate granule cell layer (top row of circles) and the band of the molecular layer. Scale bars=150 μm.

with DAPI (h-1500, Vector Laboratories, Inc., Burlingame, CA, USA). Images were acquired digitally on an Olympus BX51 fluorescent microscope with an Olympus DP 72 camera (Olympus, Tokyo, Japan). A semiquantitative densitometric measurement of immunoflorescent staining was performed. Subtraction of background was performed on captured images. Threshold was adjusted and the image was inverted black and white to clean out the white noise. Using Image J software, the mean gray value was measured in the inner and outer molecular layer of the dentate gyrus.

At high magnification, the punctuate pattern of synapsin immunofluorescence became transparent by subsiding background. DAPI counterstained images were merged with synapsin stained images to determine the granular cell layer. The density of immunofluorescence was evaluated by Image J software because the grading scale based on visual observation was not condusive to acceptable data. Briefly, as can be seen in Fig. 2, background omitted. The image was inverted to gray and white and the density of dark punctuates were measured.

Statistical analysis

The data were expressed as the mean values and their standard errors (SEM). The variables were analyzed by one-way analysis of variance (ANOVA). When a significant effect was found between groups, Tukey *post hoc* tests were performed. Semiquantitative Timm scoring system was analyzed by a nonparametric Kruskal-Wallis test followed by the Mann-Whitney U test. Nonparametric spearman correlation was performed between cumulative damage scores and optical density of Timm granules in both septal and dorsal dentate gyrus. All analyses were performed using SPSS version 16 (SPSS Inc., Chicago, IL, USA). The statistical significance level was set at $P \leq 0.05$.

Results

Descriptive analysis of neuronal damage in hippocampus

Since cell loss may contribute to changes in granule cell morphology [25], cell loss was assessed by Nissl staining. Table 1 shows the cumulative damage scores in the rostrocaudal parts of the dorsal hippocampus. The most severe cell loss was observed in the CA1 subfields. Extensive cell loss was evident in the hilus and upper blade of the dentate gyrus, as well. Scattered cell loss was observed in the CA3 pyramidale cell layer. Consequently, the highest cumulative damage score

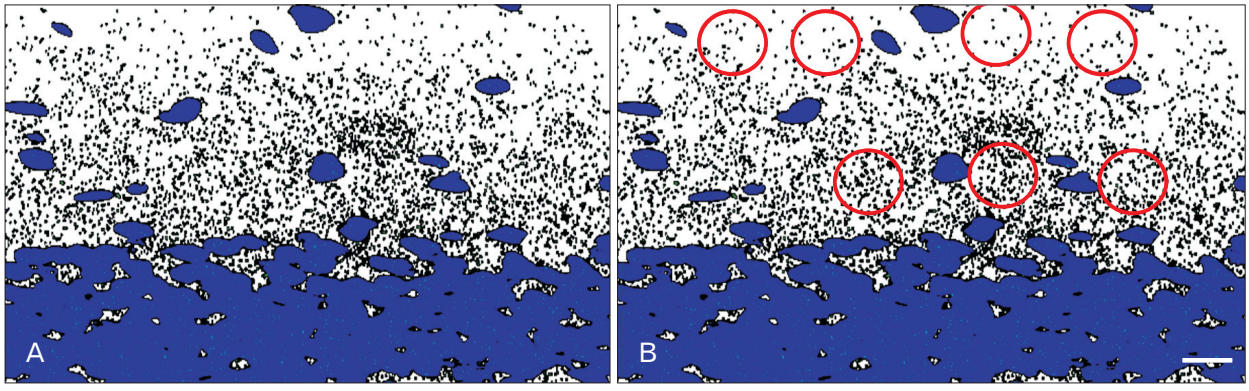

Fig. 2. Descriptive pattern of immune-densitometry process. (A) The synapsin stained taken image was converted to white and gray scale after omitting the background. DAPI stained image was merged with synapsin stained image to determine the boundary of granular layer. (B) A fixed number of circles with determined dimension was randomly placed in inner and outer molecular layers to determine the density of punctuate pattern of synapsin immunofluorescence. Scale bar=200 μm.

Table 1. Descriptive report of cumulative damage scores in the septal and temporal hippocampus

		Control	Epilepsy	Vehicle	Melatonin 5 mg/kg 60 days	Melatonin 5 mg/kg 14 days	Melatonin 20 mg/kg 60 days	Melatonin 5 mg/kg 14 days
Dorsal hippocampal cumulative damage score	Rostral part	0	0.57±0.42	0.42±0.29	0.28±0.18	0.33±0.21	0.28±0.18	0.14±0.14
	Caudal part	0	5.57±0.64	5.85±0.96	4.71±0.47	3.50±1.05	3.57±0.64	2.28±0.42

Values are expressed as mean±SEM.

http://dx.doi.org/10.5115/acb.2016.49.1.21

was calculated in the caudal part of the dorsal hippocampus. In all of the treated groups, melatonin administration reduced the cumulative damage scores along the rostro-caudal parts of the dorsal hippocampus.

Numeric quantification of neuronal cells

Numeric quantification of neuronal cells in the different layers of the hippocampus and cortical regions are shown in Table 2. We did not observed any significant differences between vehicle and epileptic animals in any analyzed region. Neuronal cell body quantification within the CA1 region of untreated epileptic animals revealed a significant neuronal loss (epilepsy group 84.85±27.96 vs. control 347.5±12.89, $P \leq 0.05$) and gliosis (SO: epilepsy group 167.51±25.58 vs. control 78.66±6.38, $P \leq 0.01$; stratum radiatum [SR]: epilepsy group 176.74±26.50 vs. control 55.16±4.79, $P \leq 0.01$) in the caudal part of the dorsal hippocampus. Neuronal dropout was also significant in the rostral part of CA1 subfield (epilepsy group 77.14±15.76 vs. control 159.33±3.22, $P \leq 0.05$). The moderate injury in the rostral part of the dorsal hippocampus in epileptic animals did not result in a significant change in cell distribution in the SO and SR layers of CA1 subfield. Melatonin treatment with 20 mg/kg dosage increased the number of CA1 neurons in the caudal part of the dorsal hippocampus in both 14 (treated group 136.14±8.81 vs. epilepsy group 77.14±15.76, $P \leq 0.01$) and 60 (treated group 135.14±10.63 vs. epilepsy group 77.14±15.76, $P \leq 0.05$) days treated groups. Significant cell loss was evident in CA3 subfields along the rostro-caudal axis of the dorsal hippocampus in untreated epileptic animals (septal part: epilepsy group 89.14±12.02 vs. control 148.66±4.75; dorsal part: epilepsy group 67.71±13.17 vs. control 147.67±10.45, $P \leq 0.01$) in comparison to control specimens. The 20 mg/kg melatonin treated groups showed a significant increase in the number of CA3 pyramidale neurons in both the rostral (14 days group, $P \leq 0.01$; 60 days group, $P \leq 0.01$) and the caudal (14 days group, $P \leq 0.001$; 60 days group, $P \leq 0.01$) parts of the hippocampus.

A significant decrease in the granular cell number was observed in the caudal part of the dorsal dentate gyrus of untreated epileptic animals (epilepsy group 693.43±33.74 vs. control 1,038.7±43.59, $P \leq 0.001$).This reduction was related to the occurrence of profound neuronal loss in the upper blade. Contrary to the dorsal part, the rostral part of the dorsal dentate gyrus of epileptic animals was resistant to neuronal injury and showed a significant increase in the granular cell number 60 days post SE (epilepsy group 762.28±28.65 vs. control 634.33±19.73, $P \leq 0.01$).

Table 2. Numeric quantification of neurons in different layers of hippocampus and cortical regions

		Control	Epilepsy	Vehicle	Melatonin 5 mg/60 days	Melatonin 5 mg/14 days	Melatonin 20 mg/60 days	Melatonin 20 mg/14 days
Rostral part of dorsal hippocampus	CA1	159.33±3.22	77.14±15.76*	75.28±13.66	109.14±19.18	99.16±8.73	136.14±8.81*	135.14±10.63**
	SO	33.66±2.04	46.71±5.59	53.14±5.07	54.28±13.09	32.33±3.24	33.85±1.89	30.14±2.22
	SR	21.16±1.24	49.71±4.94	51.14±6.64	54.57±8.76	47.16±6.40	37.71±4.76	47.28±15.91
	CA3	148.66±4.75	89.14±12.02*	93±12.28	83.28±7.15	114.66±6.76	131.57±14.40**	133±8.64**
	Hilus	41.50±3.14	43.85±2.80	41.28±2.60	44.71±2.87	45.66±2.30	47.42±3.63	37.57±2.30
	DG	634.33±19.73	762.28±28.65**	763.14±21.23	739.71±26.77	785.5±45.59	1152±46.39*	1287±46*
Caudal part of dorsal hippocampus	CA1	347.5±12.89	84.85±27.96*	82.94±44.53	110.29±27.13	174.35±39.02	137.88±39.28	165.17±32.57
	SO	78.66±6.38	167.51±25.58**	181.09±19.55	209.30±13.95	141.05±23.18	162.30±20.85	157.41±19.23
	SR	55.16±4.79	176.74±26.50**	190.20±31.05	207.34±27.59	120.93±18.09	118.73±14.92	136.43±23.04
	CA3	147.67±10.45	67.71±13.17*	67.44±10.26	94.85±6.29	98.16±15.49	106.14±9.14**	103.43±11.21***
	Hilus	34.33±2.91	38.71±4.28	34.14±3.99	40.14±2.02	42±3.42	43.14±1.33	30.14±1.99
	DG	1038.7±43.59	693.43±33.74***	707.91±18.16	1260±84.15*	1460.8±27.59*	1168.6±11.90*	1442.4±93.14*
Piriform	I	22.16±1.49	136±10.49*	123.71±19.81	120.29±9.48	88.50±19.34	126±19.22	117.57±18.68
	II	166±5.05	30.71±5.90*	31.14±7.65	12.71±3.11	55.33±13.70	37.57±24.78	15.57±3.77
	III	70.33±3.13	17.85±3.22*	14.57±5.23	3.28±.80	14.16±6.37	17.28±12.29	4.14±1.22
Dorsal entorhinal	II	24±1.21	16.42±1.75	16.57±1.28	21±2.82	17.33±1.60	20.85±1.79	18.14±.96
	III–IV	32.66±2.56	9±1.43**	5.85±1.89	18.71±2.87	18±9.69	20.71±3.61	16.28±3.61
Ventral entorhinal	II	24.33±24.33	17.16±2.62	16±2.41	20±2.75	12±1.23	16.40±1.56	13±1.08
	III–IV	25.66±1.20	12±2.84**	11.42±2.58	15.6±2.56	9.66±1.05	10.80±0.58	9.75±2.92

Values are expressed as mean±SEM. The epilepsy group was compared with the control group. The melatonin treated groups were compared to the vehicle group. There was not any significant difference between epileptic and vehicle groups. The number of neurons in melatonin treated groups were compared with the vehicle group. SO, stratum oriens; SR, stratum radiatum; DG, dendate zyrus. *$P \leq 0.05$, **$P \leq 0.01$, ***$P \leq 0.001$. ANOVA was followed by Tukey *post-hoc*.

The number of granular cells in the rostral part of the dorsal hippocampus increased significantly following 20 mg/kg melatonin treatment in both 14 (treated group 1,152±46.39 vs. epilepsy group 762.28±28.65, $P \leq 0.05$) and 60 days treated groups (treated group 1,287±46 vs. epilepsy group 762.28±28.65, $P \leq 0.05$). Interestingly, the number of granular neurons in the rostral part of the dorsal dentate gyrus of animals with 14 and 60 days 20 mg melatonin treatment showed a significant increase in comparison with intact control animals as well as both 5 mg/14 days or 60 days treated groups. In the caudal part of the dorsal dentate gyrus, the number of granular neurons showed a profound increase in all melatonin-treated groups ($P \leq 0.05$). There was not any significant difference in the number of granular neuroses between the melatonin treated groups. Epilepsy caused a significant neuronal loss in layers II (epilepsy group 30.71±5.90 vs. control 166±5.05, $P \leq 0.05$) and III (epilepsy group 17.85±3.22 vs. control 70.33±3.13, $P \leq 0.05$) of the piriform cortex in addition to layer III–IV of the temporal (epilepsy group 9±1.43 vs. control 32.66±2.56, $P \leq 0.01$) and ventral entorhinal cortices (epilepsy group 12±2.84 vs. control 25.66±1.20, $P \leq 0.01$). There was no significant overt layer II cell loss of the dorsal and ventral entorhinal cortex. Moreover, non principal neurons were distributed in the layer I of piriform cortex. Neither dose response nor time course melatonin treatment protected temporal cortices against neuronal loss.

Axonal sprouting in the dentate gyrus and CA3 subfield

We evaluated the axonal sprouting in the dentate gyrus and CA3 subfield based on both grading system (Table 3) and computational densitometry (Fig. 1). Regarding Fig. 3A–L, in the epileptic groups, an intensive labeling of Timm granules was observed in the inner molecular layer of the dentate gyrus. The dense band of aberrant sprouted mossy fibers did not extend beyond the inner molecular layer. The pattern of aberrant mossy fiber sprouting in the epileptic animals showed almost a constant distribution along the rostro-caudal parts of the hippocampus. The results of both grading system (Table 3) and computational densitometry (Fig. 3M) showed that the density of SGL Timm granules decreased significantly in the rostro-caudal parts of the dorsal hippocampus in melatonin treated groups.

As is seen in Fig. 3M, variable intensity of Timm staining was observed in the rostral part of the CA3 subfield in control animals. Increased density of Timm granules in the SO of the CA3 subfield was calculated along the rostro-caudal parts of the dorsal hippocampus in the untreated epileptic animals ($P \leq 0.05$). None of the melatonin administration schedules were able to reduce the amount of axonal sprouting in the rostro-caudal parts of the dorsal CA3 subfields.

Previously it was reported that cell loss may contribute to changes in granule cell morphology [25]. Since melatonin treatment was able to decrease the pattern of aberrant mossy fiber sprouting in parallel with changing the amount of cumulative damage score in the hippocampus, we performed Spearman correlation between the cumulative damage scores and the optical density of supragranular Timm granules for elucidating whether there would be any correlation between their fluctuations. Spearman correlation showed a similar trend between the fluctuation of cumulative damage scores and optical density of supragranular Timm granules in both the rostral (r=0.64, $P \leq 0.001$, correlation was significant at the 0.01 level) and caudal parts (r=0.28, $P \leq 0.05$) of the dorsal hippocampus.

Immunoreactivity of synapsin I

Epilepsy induced the occurrence of the synapsin I immunoreactivity in both inner and outer molecular layers of the dentate gyrus of untreated epileptic animals (Fig. 4A–F).

Table 3. Semiquantitave analysis of axonal sprouting in both the dentate gyrus and CA3 subfield along the septotemporal axis based on scoring system

	Control	Epilepsy	Vehicle	Melatonin 5 mg/60 days	Melatonin 5 mg/14 days	Melatonin 20 mg/60 days	Melatonin 20 mg/14 days
Rostral part of dorsal DG	0	4.07±0.39**	4.7±0.14	2.28±0.51*	1.83±0.7*	1.57±0.51**	1.71±0.52**
Caudal part of dorsal DG	0	4.21±0.34***	4.57±0.20	2.64±0.3*	2.5±0.6*	1.71±0.64**	1.42±0.68**
Septal CA3	0.83±0.40	4.35±0.28**	4.78±0.14	4.50±0.42	4.75±0.17	4.85±0.14	3.85±0.28
Dorsal CA3	0.5±0.34	4.57±0.20**	4.14±0.44	3.5±0.32	4.66±0.21	3.57±0.61	3.71±0.34

Values are expressed as mean±SEM. Nonparametric Kruskal-Wallis test followed with Mann-Whitney U test. The epilepsy groups were compared with the control group. There were not any significant differences between vehicle and epileptic groups. Melatonin treated groups were compared with the vehicle group. DG, dendate zyrus. *$P \leq 0.05$, **$P \leq 0.01$, ***$P \leq 0.001$.

http://dx.doi.org/10.5115/acb.2016.49.1.21

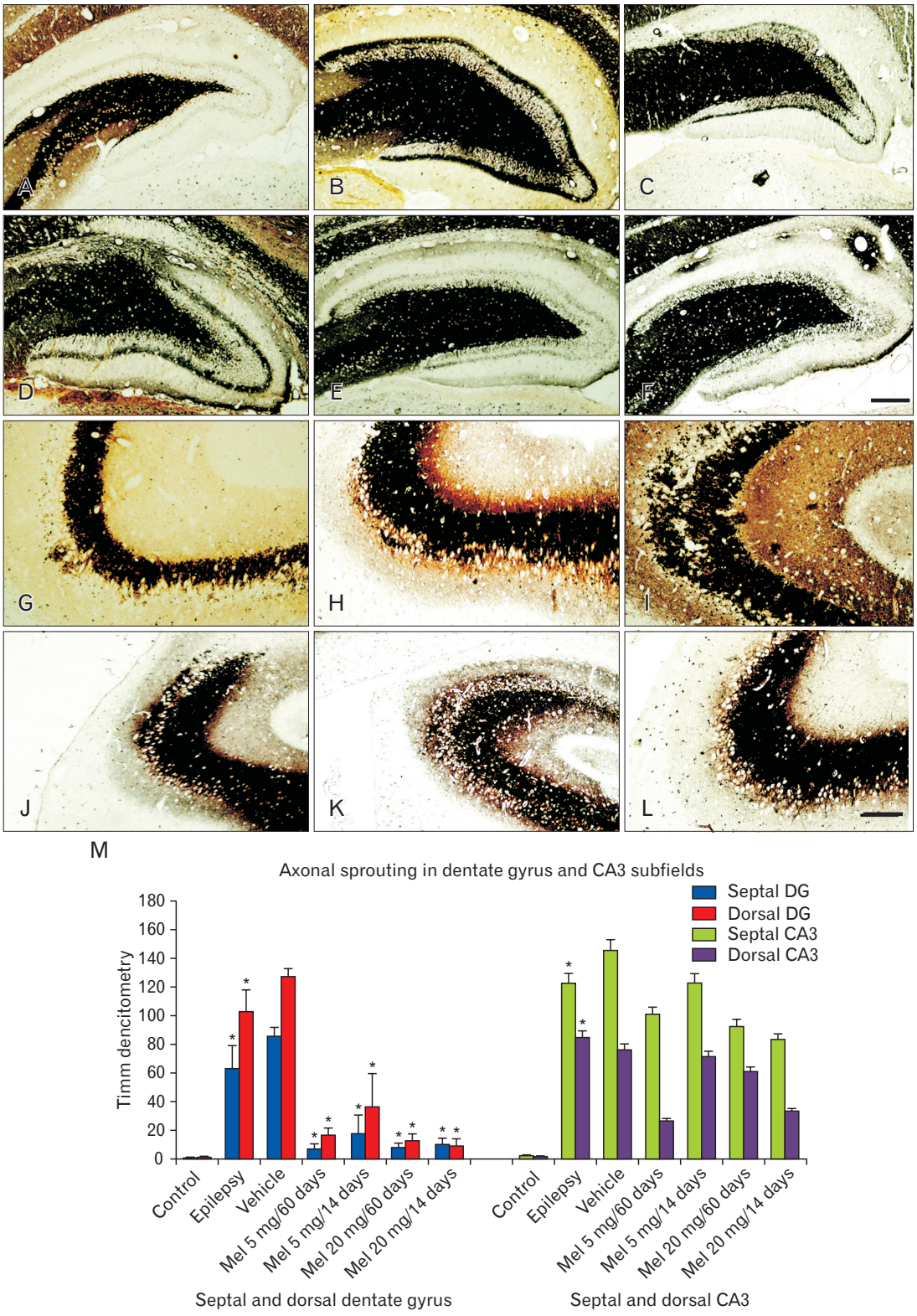

Fig. 3. (A–L) Descriptive representation of Timm staining in the caudal part of dorsal hippocampus and rostral pole of dorsal CA3 subfields. (A–F) Dentate gyrus (DG). (G–L) CA3 subfield. Control (A, G), epilepsy (B, H), 5 mg/kg for 60 days (C, I), 5 mg/kg for 14 days (D, J), 20 mg/kg for 60 days (E, K), and 20 mg/kg for 14 days (F, L). Scale bars=800 μm. (M) The density of sprouted axons in the both rostro-caudal pole of dorsal dentate gyrus in addition to CA3 subfields. The epilepsy group was compared to control one. The melatonin treated group was compared to the vehicle one. Mel, melatonin. **P*≤0.05.

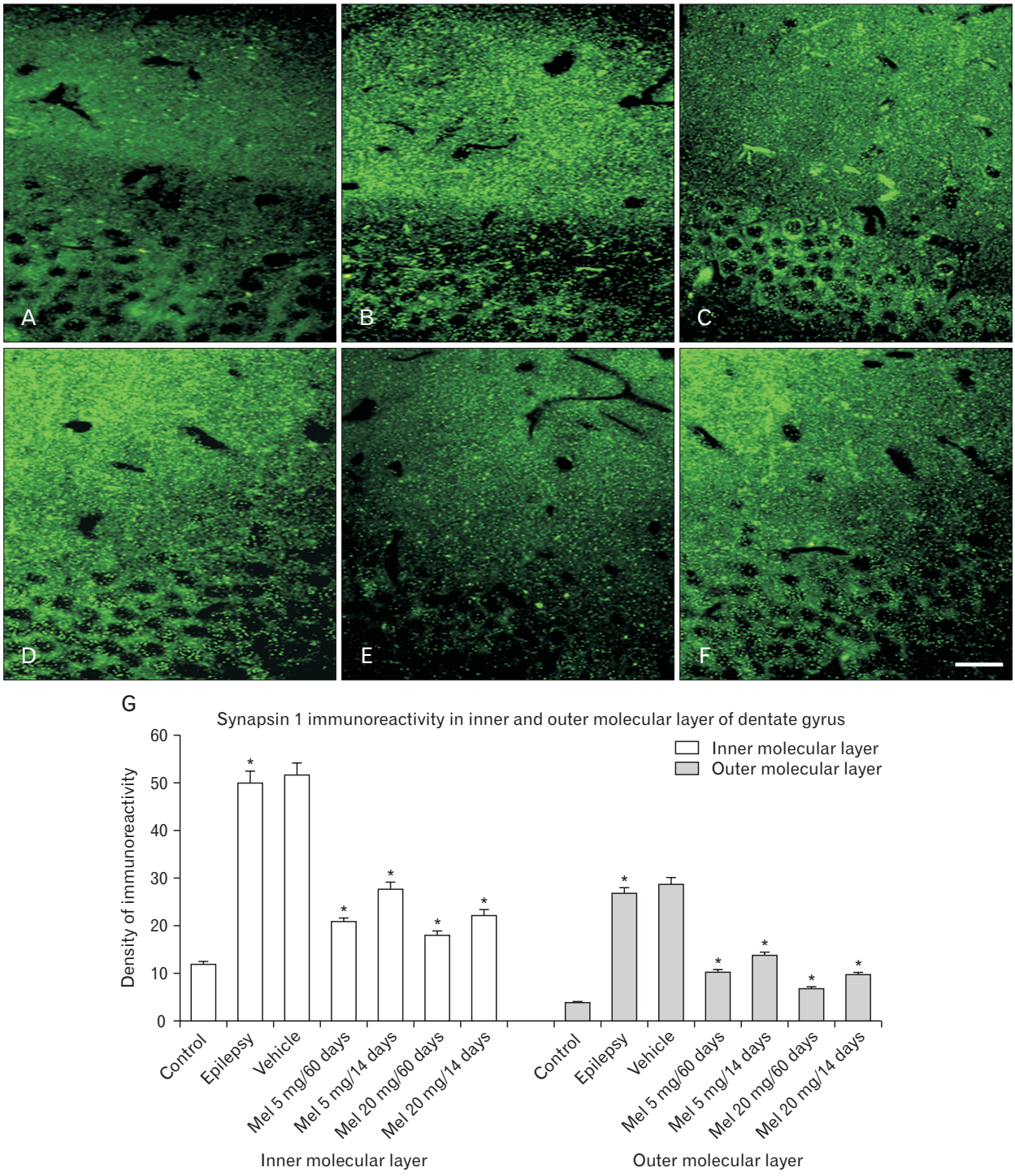

Fig. 4. (A–F) Representation of distribution of synapsin I immunoreactivity in the different layers of dorsal dentate gyrus. Control (A), epilepsy (B), 5 mg/kg melatonin for 60 days (C), 5 mg/kg melatonin for 14 days (D), 20 mg/kg melatonin for 60 days (E), and 20 mg/kg melatonin for 14 days (F). Scale bar=200 μm. (G) The quantitative densitometry of inner and outer molecular layers of dentate gyrus in the different groups. The epilepsy group was compared to control one. The melatonin treated groups were compared to sham one. Mel, melatonin. *$P \leq 0.05$.

The result of computer assisted densitometry of immunoreactivity in both the inner and outer molecular layer (Fig. 2) is represented in Fig. 4G. Epilepsy increased the density of synapsin I immunoreactivity in the inner (epilepsy 50±5.10 vs. control 12.02±1.67) and outer (epilepsy 26.73±3.21 vs. control 3.98±1.19) molecular layer of untreated epileptic

http://dx.doi.org/10.5115/acb.2016.49.1.21

animals in comparison to controls. All melatonin treated groups showed a significant decrease in the quantity of immunoreactivity in the inner molecular layer of the dentate gyrus. The pattern of vesicle distribution in outer molecular layer of the dentate gyrus changed following melatonin treatment as well (Fig. 4G). Melatonin treatment significantly reduced the immunoreactivity of outer molecular layer in all treated groups in comparison to untreated epileptic group.

Discussion

Pathomorphological consequences of TLE occur acutely and chronically after SE induction. The importance of TLE induced histological injuries is related to the probable role of different brain areas either in triggering or participating in the epileptogenic process [26, 27]. In accordance with findings of previous studies, the extension and location of neuronal loss of epileptic animals observed here were dominantly along the rostro-caudal axis of the dorsal hippocampus, all layers of the piriform cortex, and layer III–IV of the dorsal and ventral entorhinal cortices [1, 21, 34]. Neuronal death following an early neuronal stress such as SE induction can be divided to two categories. Acute and early neuronal death in the piriform and entorhinal cortices that almost fully develops by 24 hours [21]. In parallel, early neuronal injury in the granule cells of the dentate gyrus, CA1, and CA3 subfields is followed by a delayed and progressive process of neuronal death in these brain areas as well [34, 35]. The hippocampus as a heterogeneous brain area has a functional and neurotransmission dissociation along its septo-temporal axis [36, 37], it is well defined that the dorsal part is involved more in learning/memory and spatial navigation [36]. Not only was the greater susceptibility of the dorsal hippocampus against different induced brain injuries proved previously [38], but also different patterns of neuronal injury along the rostro-caudal axis of the dorsal hippocampus were observed. Although the rostral pole of the dorsal dentate gyrus showed a significant increase in untreated epileptic animals (epilepsy 762.28±28.65 vs. control 634±19.73), the caudal pole of the dorsal dentate gyrus showed a significant reduction (epilepsy 693.43±33.74 vs. control 1,038.7±43.59). Since neurogenesis in the granular layer was affirmed as a chronic consequence of SE induction [1, 30], this gradient along the rostro-caudal axis of the dorsal hippocampus can be attributed to the differential susceptibility of different subpopulations of granule cells in the suprapyramidal blade compared to the infrapyramidal blade towards neuronal injury [39]. The pattern of both the CA1 and CA3 neuronal defect was similar along the rostro-caudal axis of the dorsal hippocampus.

Region-specific effects of agomelatine and other treatments along the dorso-ventral axis of the hippocampus were studied previously [40-44]. While agomelatine can stimulate cell survival and proliferation in the dorsal hippocampus, it is discussed that cell proliferation, neurogenesis and maturation of adult newborn neurons by agomelatine is restricted to the ventral hippocampus [40, 41, 44]. Lima et al. [14] showed that melatonin administration even 30 minutes after SE induction over 48 hours (total amount, 22.5 mg/kg) can protect the CA3 subfield 60 days after the first injury. As shown in Table 2, either 14 or 60 days of high dose melatonin administration was able to preserve higher numbers of pyramidal neurons against neuronal death in both the rostral and caudal part of the dorsal CA3 subfield of treated animals in comparison to untreated epileptic ones. We observed a region-specific pattern of neuronal protection along the rostro-caudal axis of the dorsal hippocampus. In which, similarly to Lima et al. [14], lack of neuronal protection in the caudal part of the dorsal CA1 subfield was accompanied by higher number of neurons in the rostral part of the dorsal CA1 subfield following high dose melatonin treatment (20 mg/kg for 60 and 14 days, respectively; 136.18±8.81, 135.14±10.63) in comparison to the untreated epileptic group (75.28±13.66). As melatonin treatment for 14 days is not able to cause newborn neuron generation in the pyramidale layers [9], the protective effect of melatonin can be attributed to the reduction of excessive neuronal activity [14], inflammation, and oxidative stress by activating various signaling pathways following SE induction [15, 17]. The profound role of melatonin in increasing the number of dentate gyrus granular neurons in all of the melatonin treated groups was further evidence of the profound effect of prolonged neurohormone treatment in the rostro-caudal axis of the dorsal hippocampus. Although Ramirez-Rodriguez et al. [45] reported that 14 days melatonin administration is sufficient for increasing the net neurogenesis of the dentate gyrus in intact mice, Rennie et al. [9] showed that the neurogenic effect of melatonin (0.51±0.02 mg/kg/day) on the granular neurons of pinealectomized rats can just be detected over 6 months of daily treatment. Since the number of counted granular neurons in melatonin treated epileptic groups overt the quantity in untreated epileptic group and even normal group, this discrepancy may be explained by the fact that melatonin can increase the number

of surviving epilepsy induced newborn neurons rather than triggering neurogenesis because of its pleiotropic nature [9, 46]. Lack of neuronal protection in the cudal pole of the dorsal CA1 subfield, piriform, and the entorhinal cortices following post SE melatonin administration need further study to elucidate region specific and time dependent effects of melatonin on neuronal population.

Axonal reorganization is one of the main constructive features of epilepsy [25]. In accordance with previous studies [25, 32], a remarkable supragranular mossy fiber sprouting along the rostro-caudal axis of the dorsal hippocampus was observed in the epileptic group. Although mossy fiber sprouting can further trigger the occurrence of recurrent spontaneous seizures [47], it was shown that even 1- and 10-hour topiramate injection post-SE as an improved anti-convulsant drug could not stop mossy fiber sprouting as a marker of the epileptogenesis process [21]. Lima et al. [14] reported that even short term melatonin treatment (30 minutes after SE induction till 48 hours later; melatonin, 22.5 mg/kg) could reduce the grade of aberrant supragranular mossy fiber sprouting (SE group, grade 4; SE+melatonin group, grade 3) 60 days after SE induction. As supragranular mossy fiber sprouting in all melatonin treated groups of the present study scored lower than grade 3 in comparison with Lima et al. [14] scores, it can be concluded that melatonin treatment during the early and chronic phases of TLE was more efficient in reducing aberrant axonal sprouting in the dentate gyrus rather than only 48-hour postprecipitating injury. For understanding the exact mechanism of this reduction, more studies are needed.

Alteration in Timm staining of CA3 SO following SE induction [32, 48] clarified that epilepsy causes the extension of mossy fiber axons into the CA3 area [25, 32]. The sprouting can be rooted in development of new synapses in response to regression of synapses [32] and aberrant axonal sprouting of newborn granule cells into SO of CA3 [30]. Moreover, sprouting of axon collaterals by pyramidale cells of SP layer assumes as another source of SO sprouting [48]. Accordingly, a remarkable CA3 sprouting along the rostro-caudal axis of the dorsal hippocampus was observed in the untreated epileptic group. Neither dose dependent nor time window melatonin treatment was able to significantly alter the CA3 sprouting along the rostro-caudal axis of the dorsal hippocampus. Since reduced number of pyramidale cells and exceeding number of granule cells can result in CA3 mossy fiber sprouting, more research is necessary to determine the origin and involved mechanism of CA3 SO axonal sprouting and the exact effect of melatonin treatment on them.

Density quantification of synapsin I immunoreactivity showed a significant increase in the inner molecular layer of the epileptic group (Fig. 4G). This pattern of immunoreactivity is related to the aberrant mossy fiber sprouting which was detected by Timm staining as well. TLE caused the immunoreactivity of synapsin I to increase significantly in the outer molecular layer of the dentate gyrus as well. The density of immunoreactivity decreased following melatonin treatment in all of four experimental groups (Fig. 4G). Dagyte et al. [49] indicated that chronic stress may compromise synaptic transmission from the entorhinal–hippocampal projections. In response to pathophysiological conditions such as TLE, the outer molecular layer of the dentate gyrus undergoes synaptic plasticity. Both excitatory and inhibitory synapses participate in this plasticity modification [50]. Interestingly Dagyte et al. [49] revealed that agomelatine can significantly reduce the immunoreactivity of synapsine I in the hippocampus of both control and chronicly stressed animals. Because the Timm technique selectively labels zinc rich glutamatergic granules [49] rather than GABAergic vesicles, further researches are necessary to clarify the specificity of occurred synaptogenesis in the outer molecular layer of the dentate gyrus.

Taken together, long term post-lesion melatonin treatments during the early and chronic phases of TLE altered some degree of the chronic consequences of epilepsy. Rostro-caudal axis of dorsal CA3 and CA1 subfields showed a region-specific pattern following both time windows high dose melatonin treatment. The increased number of granular cells of the dentate gyrus in the chronic epileptic animals was boosted significantly following melatonin treatment. In the epileptic animals, the increased density of both aberrant sprouted mossy fibers in the inner molecular layer and vesicle content in the outer molecular layer of the dentate gyrus reduced following melatonin treatment. Melatonin neither protected piriform and enthorhinal cortices against neuronal death nor reduced CA3 axonal sprouting over 2 months of SE induction. Although we did not observe any overt histological differences between the results of 14 and 60 days melatonin administration, it remains to clarify the exact effect of melatonin treatment based on time window of latent phase. In conclusion, long-term melatonin administration as a co-adjuvant can reduce the post-lesion region-specific histological consequences of TLE in the rostro-caudal axis of the dorsal hippocampus.

http://dx.doi.org/10.5115/acb.2016.49.1.21

Acknowledgements

This work was supported by a grant from the Research vice-chancellery of Zanjan University of Medical Sciences (ZUMS). We are grateful to Dr. Astrid Nehlig (Strasbourg, France) for her worthwhile consultation and comments in the experimental procedures and manuscript preparation.

References

1. Jung KH, Chu K, Lee ST, Kim JH, Kang KM, Song EC, Kim SJ, Park HK, Kim M, Lee SK, Roh JK. Region-specific plasticity in the epileptic rat brain: a hippocampal and extrahippocampal analysis. Epilepsia 2009;50:537-49.
2. Fisher RS, van Emde Boas W, Blume W, Elger C, Genton P, Lee P, Engel J Jr. Epileptic seizures and epilepsy: definitions proposed by the International League Against Epilepsy (ILAE) and the International Bureau for Epilepsy (IBE). Epilepsia 2005;46:470-2.
3. Kwan P, Schachter SC, Brodie MJ. Drug-resistant epilepsy. N Engl J Med 2011;365:919-26.
4. Schuele SU, Lüders HO. Intractable epilepsy: management and therapeutic alternatives. Lancet Neurol 2008;7:514-24.
5. Maestroni GJ, Conti A, Pierpaoli W. Role of the pineal gland in immunity: II. Melatonin enhances the antibody response via an opiatergic mechanism. Clin Exp Immunol 1987;68:384-91.
6. Jou MJ, Peng TI, Reiter RJ, Jou SB, Wu HY, Wen ST. Visualization of the antioxidative effects of melatonin at the mitochondrial level during oxidative stress-induced apoptosis of rat brain astrocytes. J Pineal Res 2004;37:55-70.
7. Rodriguez C, Mayo JC, Sainz RM, Antolín I, Herrera F, Martín V, Reiter RJ. Regulation of antioxidant enzymes: a significant role for melatonin. J Pineal Res 2004;36:1-9.
8. Imbesi M, Uz T, Manev H. Role of melatonin receptors in the effects of melatonin on BDNF and neuroprotection in mouse cerebellar neurons. J Neural Transm (Vienna) 2008;115:1495-9.
9. Rennie K, De Butte M, Pappas BA. Melatonin promotes neurogenesis in dentate gyrus in the pinealectomized rat. J Pineal Res 2009;47:313-7.
10. Moriya T, Horie N, Mitome M, Shinohara K. Melatonin influences the proliferative and differentiative activity of neural stem cells. J Pineal Res 2007;42:411-8.
11. Ramirez-Rodriguez G, Ortíz-López L, Domínguez-Alonso A, Benítez-King GA, Kempermann G. Chronic treatment with melatonin stimulates dendrite maturation and complexity in adult hippocampal neurogenesis of mice. J Pineal Res 2011; 50:29-37.
12. Benítez-King G. Melatonin as a cytoskeletal modulator: implications for cell physiology and disease. J Pineal Res 2006;40:1-9.
13. Costa-Lotufo LV, Fonteles MM, Lima IS, de Oliveira AA, Nascimento VS, de Bruin VM, Viana GS. Attenuating effects of melatonin on pilocarpine-induced seizures in rats. Comp Biochem Physiol C Toxicol Pharmacol 2002;131:521-9.
14. Lima E, Cabral FR, Cavalheiro EA, Naffah-Mazzacoratti Mda G, Amado D. Melatonin administration after pilocarpine-induced status epilepticus: a new way to prevent or attenuate postlesion epilepsy? Epilepsy Behav 2011;20:607-12.
15. Chung SY, Han SH. Melatonin attenuates kainic acid-induced hippocampal neurodegeneration and oxidative stress through microglial inhibition. J Pineal Res 2003;34:95-102.
16. De Lima E, Soares JM Jr, del Carmen Sanabria Garrido Y, Gomes Valente S, Priel MR, Chada Baracat E, Abrão Cavalheiro E, da Graça Naffah-Mazzacoratti M, Amado D. Effects of pinealectomy and the treatment with melatonin on the temporal lobe epilepsy in rats. Brain Res 2005;1043:24-31.
17. Lee SH, Chun W, Kong PJ, Han JA, Cho BP, Kwon OY, Lee HJ, Kim SS. Sustained activation of Akt by melatonin contributes to the protection against kainic acid-induced neuronal death in hippocampus. J Pineal Res 2006;40:79-85.
18. Ravizza T, Gagliardi B, Noé F, Boer K, Aronica E, Vezzani A. Innate and adaptive immunity during epileptogenesis and spontaneous seizures: evidence from experimental models and human temporal lobe epilepsy. Neurobiol Dis 2008;29:142-60.
19. Curia G, Longo D, Biagini G, Jones RS, Avoli M. The pilocarpine model of temporal lobe epilepsy. J Neurosci Methods 2008; 172:143-57.
20. Epsztein J, Represa A, Jorquera I, Ben-Ari Y, Crépel V. Recurrent mossy fibers establish aberrant kainate receptor-operated synapses on granule cells from epileptic rats. J Neurosci 2005;25:8229-39.
21. Rigoulot MA, Koning E, Ferrandon A, Nehlig A. Neuroprotective properties of topiramate in the lithium-pilocarpine model of epilepsy. J Pharmacol Exp Ther 2004;308:787-95.
22. Frotscher M, Jonas P, Sloviter RS. Synapses formed by normal and abnormal hippocampal mossy fibers. Cell Tissue Res 2006; 326:361-7.
23. Goffin K, Nissinen J, Van Laere K, Pitkänen A. Cyclicity of spontaneous recurrent seizures in pilocarpine model of temporal lobe epilepsy in rat. Exp Neurol 2007;205:501-5.
24. Jung S, Jones TD, Lugo JN Jr, Sheerin AH, Miller JW, D'Ambrosio R, Anderson AE, Poolos NP. Progressive dendritic HCN channelopathy during epileptogenesis in the rat pilocarpine model of epilepsy. J Neurosci 2007;27:13012-21.
25. Danzer SC, He X, Loepke AW, McNamara JO. Structural plasticity of dentate granule cell mossy fibers during the development of limbic epilepsy. Hippocampus 2010;20:113-24.
26. Hsu D. The dentate gyrus as a filter or gate: a look back and a look ahead. Prog Brain Res 2007;163:601-13.
27. Stoop R, Pralong E. Functional connections and epileptic spread between hippocampus, entorhinal cortex and amygdala in a modified horizontal slice preparation of the rat brain. Eur J Neurosci 2000;12:3651-63.
28. Racine RJ. Modification of seizure activity by electrical stimulation. II. Motor seizure. Electroencephalogr Clin Neurophysiol 1972;32:281-94.
29. Zheng Y, Moussally J, Cash SS, Karnam HB, Cole AJ. Intravenous levetiracetam in the rat pilocarpine-induced status epilepticus

model: behavioral, physiological and histological studies. Neuropharmacology 2010;58:793-8.
30. Parent JM, Yu TW, Leibowitz RT, Geschwind DH, Sloviter RS, Lowenstein DH. Dentate granule cell neurogenesis is increased by seizures and contributes to aberrant network reorganization in the adult rat hippocampus. J Neurosci 1997;17:3727-38.
31. Paxinos G, Watson C. The rat brain in stereotaxic coordinates. Syndney: Academic Press; 1982.
32. Holmes GL, Sarkisian M, Ben-Ari Y, Chevassus-Au-Louis N. Mossy fiber sprouting after recurrent seizures during early development in rats. J Comp Neurol 1999;404:537-53.
33. Van der Zee CE, Rashid K, Le K, Moore KA, Stanisz J, Diamond J, Racine RJ, Fahnestock M. Intraventricular administration of antibodies to nerve growth factor retards kindling and blocks mossy fiber sprouting in adult rats. J Neurosci 1995;15(7 Pt 2):5316-23.
34. Peredery O, Persinger MA, Parker G, Mastrosov L. Temporal changes in neuronal dropout following inductions of lithium/pilocarpine seizures in the rat. Brain Res 2000;881:9-17.
35. Poirier JL, Capek R, De Koninck Y. Differential progression of Dark Neuron and Fluoro-Jade labelling in the rat hippocampus following pilocarpine-induced status epilepticus. Neuroscience 2000;97:59-68.
36. Tanti A, Belzung C. Neurogenesis along the septo-temporal axis of the hippocampus: are depression and the action of antidepressants region-specific? Neuroscience 2013;252:234-52.
37. Bragdon AC, Taylor DM, Wilson WA. Potassium-induced epileptiform activity in area CA3 varies markedly along the septotemporal axis of the rat hippocampus. Brain Res 1986;378:169-73.
38. Ashton D, Van Reempts J, Haseldonckx M, Willems R. Dorsal-ventral gradient in vulnerability of CA1 hippocampus to ischemia: a combined histological and electrophysiological study. Brain Res 1989;487:368-72.
39. Hassan AH, von Rosenstiel P, Patchev VK, Holsboer F, Almeida OF. Exacerbation of apoptosis in the dentate gyrus of the aged rat by dexamethasone and the protective role of corticosterone. Exp Neurol 1996;140:43-52.
40. Banasr M, Soumier A, Hery M, Mocaër E, Daszuta A. Agomelatine, a new antidepressant, induces regional changes in hippocampal neurogenesis. Biol Psychiatry 2006;59:1087-96.
41. Soumier A, Banasr M, Lortet S, Masmejean F, Bernard N, Kerkerian-Le-Goff L, Gabriel C, Millan MJ, Mocaer E, Daszuta A. Mechanisms contributing to the phase-dependent regulation of neurogenesis by the novel antidepressant, agomelatine, in the adult rat hippocampus. Neuropsychopharmacology 2009;34:2390-403.
42. Paizanis E, Renoir T, Lelievre V, Saurini F, Melfort M, Gabriel C, Barden N, Mocaër E, Hamon M, Lanfumey L. Behavioural and neuroplastic effects of the new-generation antidepressant agomelatine compared to fluoxetine in glucocorticoid receptor-impaired mice. Int J Neuropsychopharmacol 2010;13:759-74.
43. Morley-Fletcher S, Mairesse J, Soumier A, Banasr M, Fagioli F, Gabriel C, Mocaer E, Daszuta A, McEwen B, Nicoletti F, Maccari S. Chronic agomelatine treatment corrects behavioral, cellular, and biochemical abnormalities induced by prenatal stress in rats. Psychopharmacology (Berl) 2011;217:301-13.
44. Rainer Q, Xia L, Guilloux JP, Gabriel C, Mocaër E, Hen R, Enhamre E, Gardier AM, David DJ. Beneficial behavioural and neurogenic effects of agomelatine in a model of depression/anxiety. Int J Neuropsychopharmacol 2012;15:321-35.
45. Ramírez-Rodríguez G, Klempin F, Babu H, Benítez-King G, Kempermann G. Melatonin modulates cell survival of new neurons in the hippocampus of adult mice. Neuropsychopharmacology 2009;34:2180-91.
46. Parent JM, Elliott RC, Pleasure SJ, Barbaro NM, Lowenstein DH. Aberrant seizure-induced neurogenesis in experimental temporal lobe epilepsy. Ann Neurol 2006;59:81-91.
47. Lynch M, Sutula T. Recurrent excitatory connectivity in the dentate gyrus of kindled and kainic acid-treated rats. J Neurophysiol 2000;83:693-704.
48. Siddiqui AH, Joseph SA. CA3 axonal sprouting in kainate-induced chronic epilepsy. Brain Res 2005;1066:129-46.
49. Dagyte G, Luiten PG, De Jager T, Gabriel C, Mocaër E, Den Boer JA, Van der Zee EA. Chronic stress and antidepressant agomelatine induce region-specific changes in synapsin I expression in the rat brain. J Neurosci Res 2011;89:1646-57.
50. Thind KK, Yamawaki R, Phanwar I, Zhang G, Wen X, Buckmaster PS. Initial loss but later excess of GABAergic synapses with dentate granule cells in a rat model of temporal lobe epilepsy. J Comp Neurol 2010;518:647-67.